








COMPUTATIONAL STUDY OF DRUG DELIVERY SYSTEMS WITH RADIONUCLIDE AND FLUORESCENCE IMAGING MODALITIES.

IV. DOXORUBICIN DELIVERY SYSTEMS BASED ON ALBUMIN AND HEMOGLOBIN

 V. Trusova^{a*},  U. Malovytsia^a,  P. Kuznietsov^b,  I. Yakymenko^b, I. Karnaukhov^c,
 A. Zelinsky^c,  B. Borts^c, I. Ushakov^c, L. Sidenko^c,  G. Gorbenko^a

^aDepartment of Medical Physics and Biomedical Nanotechnologies, V.N. Karazin Kharkiv National University
 4 Svobody Sq., Kharkiv, 61022, Ukraine

^bO.I. Akhiezer Department for Nuclear Physics and High Energy Physics, V.N. Karazin Kharkiv National University
 4 Svobody Sq., Kharkiv, 61022, Ukraine

^cNational Science Center "Kharkiv Institute of Physics and Technology", Kharkiv, Ukraine

*Corresponding Author E-mail: valerija.trusova@karazin.ua

Received June 2, 2025, revised July 29, 2025; accepted August 21, 2025

The development of multifunctional drug delivery systems that integrate therapeutic and diagnostic capabilities remains a major challenge in oncology. In the present work we investigated hybrid carriers composed of human serum albumin and hemoglobin (HSA-Hb) for doxorubicin (DOX) delivery combined with radionuclide and fluorescence imaging. Using molecular docking simulations, we systematically evaluated the interactions of HSA-Hb assemblies with twelve technetium-99m (^{99m}Tc)-labeled radiopharmaceuticals, DOX, and four near-infrared (NIR) dyes. The results revealed that hemoglobin markedly expands the binding landscape, providing exclusive and high-affinity sites for several ^{99m}Tc complexes (notably TcMEB and TcDIS), while also serving as the primary scaffold for DOX and NIR dyes. Two distinct DOX-binding pockets were identified within Hb subunits, suggesting enhanced drug stability and potential responsiveness to tumor hypoxia. Fluorescent dyes, including methylene blue, indocyanine green, AK7-5, and SQ1, exhibited preferential binding to Hb with affinities higher than those observed for albumin, indicating superior suitability for optical imaging. Importantly, the partitioning of radiopharmaceuticals to albumin and therapeutic/imaging ligands to hemoglobin reduced binding competition and enabled the simultaneous integration of multimodal functions within a single construct. These findings highlight HSA-Hb nanocarriers as promising candidates for next-generation theranostic platforms, combining efficient DOX delivery with non-invasive radionuclide and fluorescence monitoring.

Keywords: Protein-based drug delivery nanosystems, Human serum albumin, Hemoglobin, Doxorubicin, Technetium complexes, Near infrared dyes, Molecular docking

PACS: 87.14.C++c, 87.16.Dg

Advancing the design of multifunctional drug delivery systems remains a pivotal objective in oncological research, particularly when addressing the therapeutic limitations of cytotoxic agents such as doxorubicin (DOX) [1,2]. The challenge lies in achieving targeted delivery with minimal off-target effects, while simultaneously enabling real-time visualization of drug distribution [3]. Protein-based nanocarriers have garnered significant attention due to their favorable pharmacological profiles, including biodegradability, low immunogenicity, and the ability to accommodate both therapeutic and diagnostic payloads. Among these, human serum albumin (HSA) continues to serve as a cornerstone in drug delivery strategies, owing to its high binding capacity, extended systemic half-life, and preferential accumulation in tumor tissues via the enhanced permeability and retention (EPR) effect [4]. Building upon our prior investigations into albumin-based hybrid systems incorporating transferrin or lysozyme [5-7], we now turn our focus to hemoglobin (Hb) as a co-carrier in the development of DOX delivery platforms. Hemoglobin, a tetrameric metalloprotein with intrinsic oxygen-carrying functionality, presents unique physicochemical properties that may be harnessed for drug encapsulation and release [8]. Its quaternary structure, redox-active heme groups, and responsiveness to pH and oxidative stress render it a compelling candidate for tumor-targeted delivery, particularly in hypoxic microenvironments where conventional carriers may falter. In this study, we employ computational modeling techniques to elucidate the molecular architecture and binding energetics of DOX within albumin-hemoglobin hybrid systems. Furthermore, we investigate the feasibility of integrating radionuclide and fluorescent imaging modalities into the carrier architecture, aiming to establish a dual-functional system capable of both therapeutic action and non-invasive biodistribution tracking. Through this approach, we seek to expand the repertoire of protein-based theranostic agents and contribute to the rational design of next-generation delivery vehicles tailored for precision oncology.

METHODS

To construct the protein-based drug delivery systems (PDDS), the dimeric structure of human serum albumin (HSA) was utilized as the foundational scaffold, retrieved from the Protein Data Bank (PDB ID: 1AO6). Hemoglobin (Hb, human deoxyhemoglobin, PDB ID: 2DN2) was introduced as a secondary protein component to explore its potential synergistic

role in doxorubicin (DOX) transport and imaging agent integration. A panel of twelve technetium-99m-labeled radiopharmaceuticals was selected to evaluate the compatibility of the PDDS with nuclear imaging modalities. Complete characteristics as well as the structures of the employed complexes are given in [5-7]. To enable dual-modality imaging, these radiotracers were paired with four near-infrared (NIR) fluorescent dyes: methylene blue (MB), indocyanine green (IG), cyanine derivative AK7-5, and squaraine-based SQ1. Molecular docking simulations were performed using the HDOCK platform to identify favorable interaction sites for DOX, technetium-labeled compounds, and NIR dyes within the HSA-Hb assemblies. Ligand structures were generated using MarvinSketch (version 18.10.0) and subsequently refined through energy minimization in Avogadro (version 1.1.0). The resulting docking poses were visualized and examined using UCSF Chimera (version 1.14), and protein-ligand interactions were further characterized using the Protein-Ligand Interaction Profiler tool [9].

RESULTS AND DISCUSSION

Our previous investigations have examined the versatility of albumin-centered drug delivery platforms for transporting doxorubicin (DOX), particularly in combination with technetium-99m-based radiotracers (TCC) and near-infrared (NIR) fluorescent dyes to enable multimodal imaging [5-7]. In our initial study, human serum albumin (HSA) was identified as a robust carrier capable of forming stable complexes with both radionuclide agents and optical probes. Computational analyses, including molecular docking and short-timescale molecular dynamics simulations, confirmed the structural integrity and high-affinity interactions of these hybrid nanocarriers, underscoring their potential for theranostic applications. Building upon this framework, subsequent works expanded the carrier design by introducing transferrin (TRF) and lysozyme (Lz) as auxiliary protein partners to albumin, thereby probing their capacity to enhance tumor targeting and cellular uptake. Both HSA-TRF and HSA-Lz hybrid platforms demonstrated preserved compatibility with TCC agents and NIR dyes, confirming their potential to optimize the therapeutic precision and overall performance of DOX delivery systems. In continuation of this line of research, the present study directs attention to albumin-hemoglobin (HSA-Hb) assemblies. By characterizing their molecular interactions with DOX, technetium-based radiopharmaceuticals, and fluorescent probes, we evaluate the suitability of HSA-Hb complexes as next-generation multimodal carriers. Particular emphasis is placed on binding energetics, conformational stability, and their potential to advance the dual goals of effective therapy and non-invasive imaging.

Molecular docking simulations revealed a distinct hierarchy in the binding affinities of technetium-99m-labeled compounds (TCC) to the HSA-Hb complexes (Fig. 1, left panel). Analysis of the best docking scores (BDS) indicated that TcHYN exhibited the strongest interaction, followed by TcDIS, TcDTPA, and TcMEB.

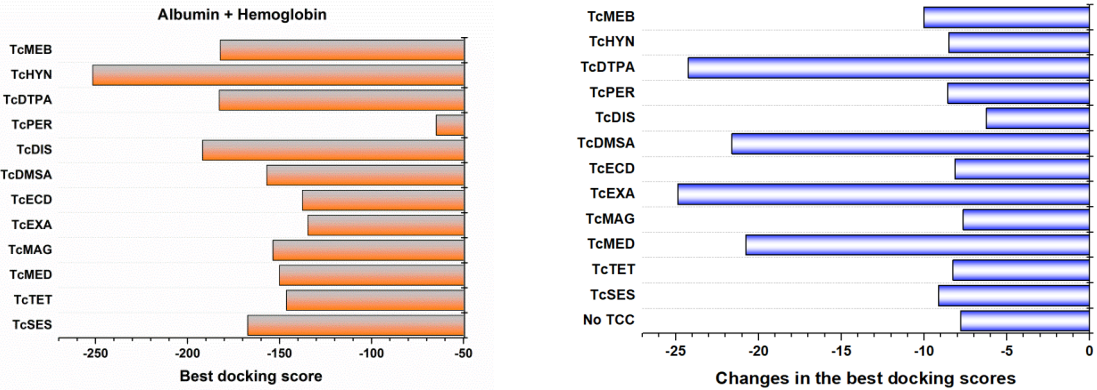


Figure 1. Absolute values (left panel) and changes (right panel) in the best docking score values obtained for the TCC complexes with HSA in the absence and presence of Hb

Intermediate affinities were observed for TcSES, TcDMSA, TcMAG, and TcMED, while TcTET, TcECD, TcEXA, and TcPER showed comparatively weaker binding. The top BDS values for HSA-Hb complexes reached -251.54, corresponding to 38 interface residues contributing to ligand stabilization (Table 1).

Table 1. The interface amino acid residues and the types of interactions involved in the binding of technetium 99m complexes (TCC) to the albumin-hemoglobin (Hb) associates

TCC	HSA-Hb-TCC interface residues			Type of interactions
	HSA	Hb		
TcSES		ASP _{99B} *, ARG _{104B} , HSD _{143B} , PRO _{37C} , ARG _{104D} , ALA _{128D} , VAL _{134D}	PRO _{100B} , ASN _{139B} , TYR _{145B} , LEU _{100C} , LEU _{105D} , GLN _{131D} , ALA _{135D} , ASN _{139D}	GLU _{101B} , ALA _{142B} , PHE _{36C} , GLU _{101D} , ASN _{108D} , LYS _{132D}
				Hydrophobic interactions, hydrogen bonds

TCC	HSA-Hb-TCC interface residues		Type of interactions
	HSA	Hb	
TcTET		GLN _{39B} , ARG _{40B} , GLU _{43B} , HSD _{97B} , PRO _{44C} , ARG _{92C}	Hydrophobic interactions
TcMED	ALA _{300B} , ASP _{301B} , LEU _{302B}	THR _{38A} , THR _{41A} , TYR _{42A} , LEU _{28D} , LEU _{31D} , LEU _{32D} , THR _{38D} , PHE _{41D} , PHE _{42D} , HSD _{63D} , VAL _{67D} , LEU _{96D} , HSD _{97D} , VAL _{98D} , ASP _{99D} , ASN _{102D} , PHE _{103D} , LEU _{106D}	Hydrogen bonds
TcMAG	ALA _{300B} , ASP _{301B}	THR _{41A} , TYR _{42A} , LEU _{28D} , LEU _{31D} , LEU _{32D} , THR _{38D} , PHE _{41D} , PHE _{42D} , HSD _{63D} , VAL _{67D} , HSD _{97D} , VAL _{98D} , ASP _{99D} , ASN _{102D}	Hydrogen bonds
TcEXA	LEU _{115A} , VAL _{116A} , ARG _{117A} , PRO _{118A} , MET _{123A} , PHE _{134A} , LYS _{137A} , TYR _{138A} , LEU _{139A} , GLU _{141A} , ILE _{142A} , ARG _{145A} , TYR _{161A} , PHE _{165A} , LEU _{182A} , ARG _{186A}		Hydrophobic interactions, hydrogen bonds
TcECD	LEU _{115B} , ARG _{117B} , PRO _{118B} , MET _{123B} , PHE _{134B} , LYS _{137B} , TYR _{138B} , GLU _{141B} , ILE _{142B} , TYR _{161B} , LEU _{182B} , ASP _{183B} , LEU _{185B} , ARG _{186B}		Hydrophobic interactions, hydrogen bonds, salt bridges
TcDMSA	LEU _{115A} , VAL _{116A} , ARG _{117A} , PRO _{118A} , MET _{123A} , TYR _{138A} , ILE _{142A} , HSD _{146A} , PHE _{149A} , LEU _{154A} , PHE _{157A} , TYR _{161A} , LEU _{182A} , LEU _{185A} , ARG _{186A} , ASP _{187A} , GLU _{188A} , GLY _{189A} , LYS _{190A}		Hydrogen bonds, salt bridges
TcDIS		PRO _{37A} , THR _{38A} , GLN _{131B} , LYS _{132B} , ALA _{135B} , ASN _{139B} , ASN _{139D} , ALA _{142D}	Hydrophobic interactions, hydrogen bonds, salt bridges
TcPER	ALA _{26B} , TYR _{30B} , LEU _{66B} , HSD _{67B} , PHE _{70B} , GLY _{71B} , ASN _{99B} , HSP _{247B} , GLY _{248B} , ASP _{249B} , LEU _{250B}		Hydrogen bonds
TcDTPA	LEU _{115A} , VAL _{116A} , ARG _{117A} , PRO _{118A} , MET _{123A} , PHE _{134A} , LEU _{135A} , LYS _{137A} , TYR _{138A} , GLU _{141B} , ILE _{142B} , TYR _{161A} , LEU _{182A} , ARG _{186A}		Hydrogen bonds, salt bridges
TcHYN	GLU _{383A} , LEU _{387A} , ASN _{391A} , LEU _{394A} , LEU _{430A} , LEU _{453A} , SER _{489A} , GLU _{492A} , ALA _{406A} , LEU _{407A} , VAL _{409A} , ARG _{410A} , TYR _{411A} , LYS _{541A} , GLU _{542A} , LYS _{545A}		Hydrogen bonds, π -stacking, salt bridges
TcMEB		LEU _{34A} , SER _{35A} , PHE _{36A} , PRO _{37A} , THR _{38A} , VAL _{1B} , GLN _{131B} , LYS _{132B} , ALA _{135B} , ASN _{139B} , PRO _{100D} , ARG _{104D} , ALA _{138D} , ASN _{139D} , ALA _{142D} , HSD _{143D} , LYS _{144D} , TYR _{145D} , HSD _{146D}	Hydrophobic interactions, hydrogen bonds

*A, B, C, D denote hemoglobin subunits

The incorporation of hemoglobin into the albumin scaffold significantly altered the ligand-binding landscape. Notably, the presence of Hb enhanced the binding affinity for several TCC agents, particularly TcMEB and TcDIS, suggesting that Hb introduces novel interaction sites or stabilizes conformational states favorable for ligand accommodation. Moderate affinity improvements were also observed for TcSES, TcMAG, and TcMED when bound to Hb-containing assemblies. Interestingly, four radiopharmaceuticals, TcSES, TcTET, TcMEB, and TcDIS, exhibited exclusive binding to the Hb component within the HSA-Hb complex (Fig. 2), with affinities surpassing those observed for albumin alone (Fig. 1, right panel).

This selective binding implies that hemoglobin not only complements HSA carrier function but may also serve as a primary docking site for certain radiopharmaceuticals. From a mechanistic perspective, tetrameric structure of Hb and its diverse subunit interfaces likely contribute to the formation of deeper or more electrostatically favorable pockets for TCC binding. Moreover, the redox-active nature of the heme groups may influence the local electronic environment, potentially stabilizing technetium complexes through transient coordination or polar interactions. These findings underscore the value of hemoglobin as a co-carrier in multimodal drug delivery systems, particularly for radiolabeled agents.

To assess the therapeutic potential of the HSA-Hb platform, we constructed ternary complexes by docking doxorubicin (DOX) onto the most favorable protein-TCC assemblies. The results revealed that DOX binding was significantly influenced by the presence of hemoglobin. Specifically, systems containing TcDTPA, TcDMSA, TcEXA,

and TcMED exhibited marked increases in DOX affinity when Hb was present. This suggests a cooperative effect, where the initial TCC binding induces conformational changes or exposes cryptic sites on Hb that are conducive to DOX interaction. In contrast, lysozyme-based systems analyzed in previous studies [5-7] showed only modest improvements in DOX binding, limited to TcTET and TcMED complexes. This comparison highlights the superior adaptability of hemoglobin in accommodating multiple ligands simultaneously, likely due to its larger surface area and more flexible quaternary structure.

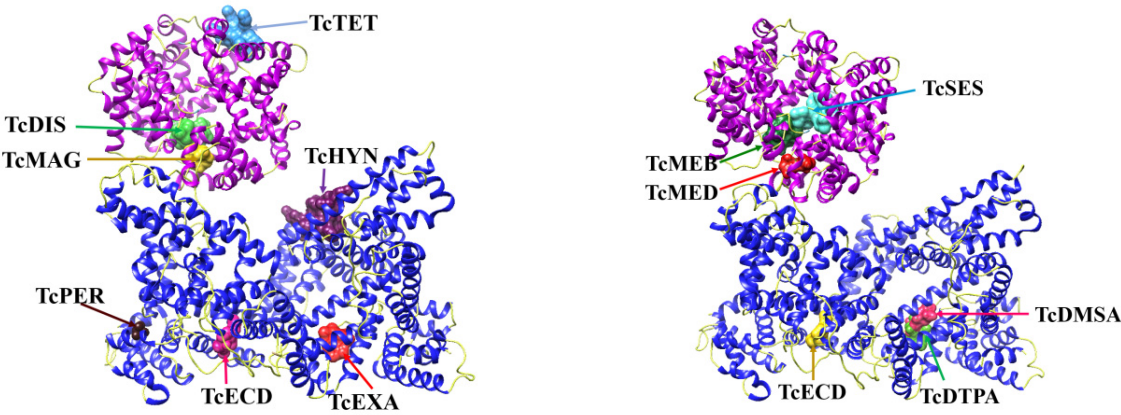


Figure 2. Best docking poses for TCC complexation with HSA-Hb systems

Detailed mapping of DOX binding sites within the HSA-Hb complexes revealed two distinct regions, both located exclusively on the hemoglobin molecule. The first site, observed in TcDIS and TcMEB systems, involved 15 residues from the A, B, and D subunits. The second, more extensive site, present in all other ternary complexes, comprised 25 residues spanning the A, B, and C subunits (Fig. 3; Table 2). These sites are likely stabilized by a combination of hydrophobic interactions and hydrogen bonding, facilitated by the amphipathic nature of DOX and the diverse chemical environment of Hb.

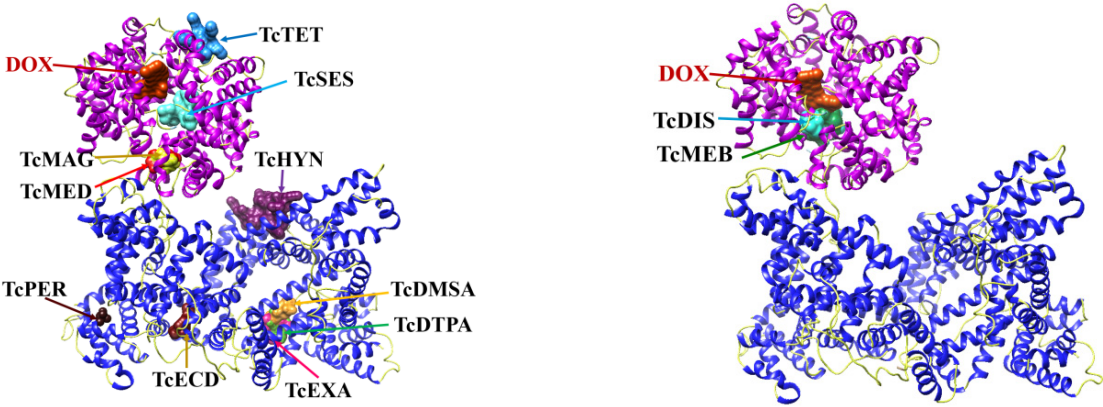


Figure 3. The highest affinity binding sites for DOX in HSA-Hb assemblies

Functionally, this Hb-mediated interaction may have twofold significance. First, Hb could act as a stabilizing scaffold that shields DOX from premature release in circulation, potentially lowering systemic toxicity. Second, the multivalent subunit interactions may facilitate drug retention within the hypoxic tumor microenvironment, where Hb oxygen-binding properties could further influence drug pharmacodynamics.

Table 2. The interface amino acid residues and the types of interactions involved in the binding of DOX to HSA-Hb-TCC complexes

Complex	HSA-Hb-TCC-DOX interface residues		Type of interactions
	HSA	Hb	
HSA-Hb-DOX		VAL _{1A} *, LEU _{2A} , LYS _{99A} , LEU _{100A} , SER _{102A} , HSD _{103A} , LEU _{106A} , ASP _{126A} , LYS _{127A} , ALA _{130A} , SER _{131A} , TYR _{35B} , TRP _{37B} , GLU _{101B} , LEU _{105B} , ASN _{108B} , ASP _{94C} , PRO _{95C} , VAL _{96C} , THR _{137C} , SER _{138C} , LYS _{139C} , TYR _{140C} , ARG _{141C}	Hydrophobic interactions, hydrogen bonds
HSA-Hb-TcSES-DOX		VAL _{1A} , LEU _{2A} , LYS _{99A} , LEU _{100A} , SER _{102A} , HSD _{103A} , LEU _{106A} , ASP _{126A} , LYS _{127A} , ALA _{130A} , SER _{131A} , TYR _{35B} , TRP _{37B} , GLU _{101B} , LEU _{105B} , ASN _{108B} , ASP _{94C} , PRO _{95C} , VAL _{96C} , THR _{137C} , SER _{138C} , LYS _{139C} , TYR _{140C} , ARG _{141C}	Hydrophobic interactions, hydrogen bonds

Complex	HSA-Hb-TCC-DOX interface residues		Type of interactions
	HSA	Hb	
HSA-Hb-TcTET-DOX		VAL _{1A} , LEU _{2A} , LYS _{99A} , LEU _{100A} , SER _{102A} , HSD _{103A} , LEU _{106A} , ASP _{126A} , LYS _{127A} , ALA _{130A} , SER _{131A} , TYR _{35B} , TRP _{37B} , GLU _{101B} , LEU _{105B} , ASN _{108B} , ASP _{94C} , PRO _{95C} , VAL _{96C} , THR _{137C} , SER _{138C} , LYS _{139C} , TYR _{140C} , ARG _{141C}	Hydrophobic interactions, hydrogen bonds
HSA-Hb-TcMED-DOX		VAL _{1A} , LEU _{2A} , LYS _{99A} , LEU _{100A} , SER _{102A} , HSD _{103A} , LEU _{106A} , ASP _{126A} , LYS _{127A} , ALA _{130A} , SER _{131A} , TYR _{35B} , TRP _{37B} , GLU _{101B} , LEU _{105B} , ASN _{108B} , ASP _{94C} , PRO _{95C} , VAL _{96C} , THR _{137C} , SER _{138C} , LYS _{139C} , TYR _{140C} , ARG _{141C}	Hydrophobic interactions, hydrogen bonds
HSA-Hb-TcMAG-DOX		VAL _{1A} , LEU _{2A} , LYS _{99A} , LEU _{100A} , SER _{102A} , HSD _{103A} , LEU _{106A} , ASP _{126A} , LYS _{127A} , ALA _{130A} , SER _{131A} , TYR _{35B} , TRP _{37B} , GLU _{101B} , LEU _{105B} , ASN _{108B} , ASP _{94C} , PRO _{95C} , VAL _{96C} , LYS _{99C} , THR _{137C} , SER _{138C} , LYS _{139C} , TYR _{140C} , ARG _{141C}	Hydrophobic interactions, hydrogen bonds
HSA-Hb-TcEXA-DOX		VAL _{1A} , LEU _{2A} , LYS _{99A} , LEU _{100A} , SER _{102A} , HSD _{103A} , LEU _{106A} , ASP _{126A} , LYS _{127A} , ALA _{130A} , SER _{131A} , TYR _{35B} , TRP _{37B} , GLU _{101B} , LEU _{105B} , ASN _{108B} , ASP _{94C} , PRO _{95C} , VAL _{96C} , THR _{137C} , SER _{138C} , LYS _{139C} , TYR _{140C} , ARG _{141C}	Hydrophobic interactions, hydrogen bonds
HSA-Hb-TcECD-DOX		VAL _{1A} , LEU _{2A} , LYS _{99A} , LEU _{100A} , SER _{102A} , HSD _{103A} , LEU _{106A} , ASP _{126A} , LYS _{127A} , ALA _{130A} , SER _{131A} , TYR _{35B} , TRP _{37B} , GLU _{101B} , LEU _{105B} , ASN _{108B} , ASP _{94C} , PRO _{95C} , VAL _{96C} , THR _{137C} , SER _{138C} , LYS _{139C} , TYR _{140C} , ARG _{141C}	Hydrophobic interactions, hydrogen bonds
HSA-Hb-TcDMSA-DOX		VAL _{1A} , LEU _{2A} , LYS _{99A} , LEU _{100A} , SER _{102A} , HSD _{103A} , LEU _{106A} , ASP _{126A} , LYS _{127A} , ALA _{130A} , SER _{131A} , TYR _{35B} , TRP _{37B} , GLU _{101B} , LEU _{105B} , ASN _{108B} , ASP _{94C} , PRO _{95C} , VAL _{96C} , THR _{137C} , SER _{138C} , LYS _{139C} , TYR _{140C} , ARG _{141C}	Hydrophobic interactions, hydrogen bonds
HSA-Hb-TcDIS-DOX		PHE _{36A} , LYS _{99A} , LEU _{100A} , SER _{102A} , HSD _{103A} , ASP _{126A} , TYR _{35B} , GLU _{101B} , ARG _{104B} , LEU _{105B} , ASN _{108B} , GLN _{131B} , VAL _{134B} , ALA _{135B} , GLU _{101D}	Hydrophobic interactions, hydrogen bonds
HSA-Hb-TcPER-DOX		VAL _{1A} , LEU _{2A} , LYS _{99A} , LEU _{100A} , SER _{102A} , HSD _{103A} , LEU _{106A} , ASP _{126A} , LYS _{127A} , ALA _{130A} , SER _{131A} , TYR _{35B} , TRP _{37B} , GLU _{101B} , LEU _{105B} , ASN _{108B} , ASP _{94C} , PRO _{95C} , VAL _{96C} , THR _{137C} , SER _{138C} , LYS _{139C} , TYR _{140C} , ARG _{141C}	Hydrophobic interactions, hydrogen bonds
HSA-Hb-TcDTPA-DOX		VAL _{1A} , LEU _{2A} , LYS _{99A} , LEU _{100A} , SER _{102A} , HSD _{103A} , LEU _{106A} , ASP _{126A} , LYS _{127A} , ALA _{130A} , SER _{131A} , TYR _{35B} , TRP _{37B} , GLU _{101B} , LEU _{105B} , ASN _{108B} , ASP _{94C} , PRO _{95C} , VAL _{96C} , THR _{137C} , SER _{138C} , LYS _{139C} , TYR _{140C} , ARG _{141C}	Hydrophobic interactions, hydrogen bonds
HSA-Hb-TcHYN-DOX		VAL _{1A} , LEU _{2A} , LYS _{99A} , LEU _{100A} , SER _{102A} , HSD _{103A} , LEU _{106A} , ASP _{126A} , LYS _{127A} , ALA _{130A} , SER _{131A} , TYR _{35B} , TRP _{37B} , GLU _{101B} , LEU _{105B} , ASN _{108B} , ASP _{94C} , PRO _{95C} , VAL _{96C} , THR _{137C} , SER _{138C} , LYS _{139C} , TYR _{140C} , ARG _{141C}	Hydrophobic interactions, hydrogen bonds
HSA-Hb-TcMEB-DOX		PHE _{36A} , LYS _{99A} , LEU _{100A} , SER _{102A} , HSD _{103A} , ASP _{126A} , TYR _{35B} , GLU _{101B} , ARG _{104B} , LEU _{105B} , ASN _{108B} , GLN _{131B} , VAL _{134B} , ALA _{135B} , GLU _{101D}	Hydrophobic interactions, hydrogen bonds

To assess the feasibility of multimodal imaging, the ternary HSA-Hb-TCC-DOX systems were subsequently docked with four near-infrared dyes: methylene blue (MB), indocyanine green (IG), AK7-5, and squaraine SQ1. The results underscored that the incorporation of Hb reshaped fluorophore binding preferences relative to albumin-only carriers. For MB, the canonical albumin binding site encompassing residues LEU115-ARG186 (site HSA115-186) was preserved in HSA-DOX and HSA-TCC-DOX complexes (Fig. 4). However, in HSA-Hb hybrids, MB predominantly engaged residues from both proteins, suggesting cooperative binding interfaces. Interestingly, MB affinity generally increased in HSA-Hb complexes compared to albumin alone, with exceptions observed in systems containing TcMED, TcEXA, TcDMSA, and TcDTPA.

In contrast, IG exhibited exclusive interactions with Hb, binding primarily within a site composed of 20 amino acids from the A, C, and D subunits (Fig. 5). Moreover, IG affinity was consistently higher in Hb-containing systems compared to albumin, highlighting hemoglobin as a superior scaffold for NIR dye incorporation. A similar trend was observed for the emerging fluorophores AK7-5 and SQ1 (data not shown), whose binding pockets were localized exclusively on Hb subunits.

This preferential dye association with hemoglobin is particularly noteworthy for theranostic design. By concentrating fluorescent reporters on Hb subunits, the hybrid carriers may achieve enhanced optical signal intensity and improved imaging contrast. Additionally, the spatial segregation of DOX and fluorophores within different Hb domains could reduce steric hindrance, ensuring that therapeutic and diagnostic functions are maintained simultaneously.

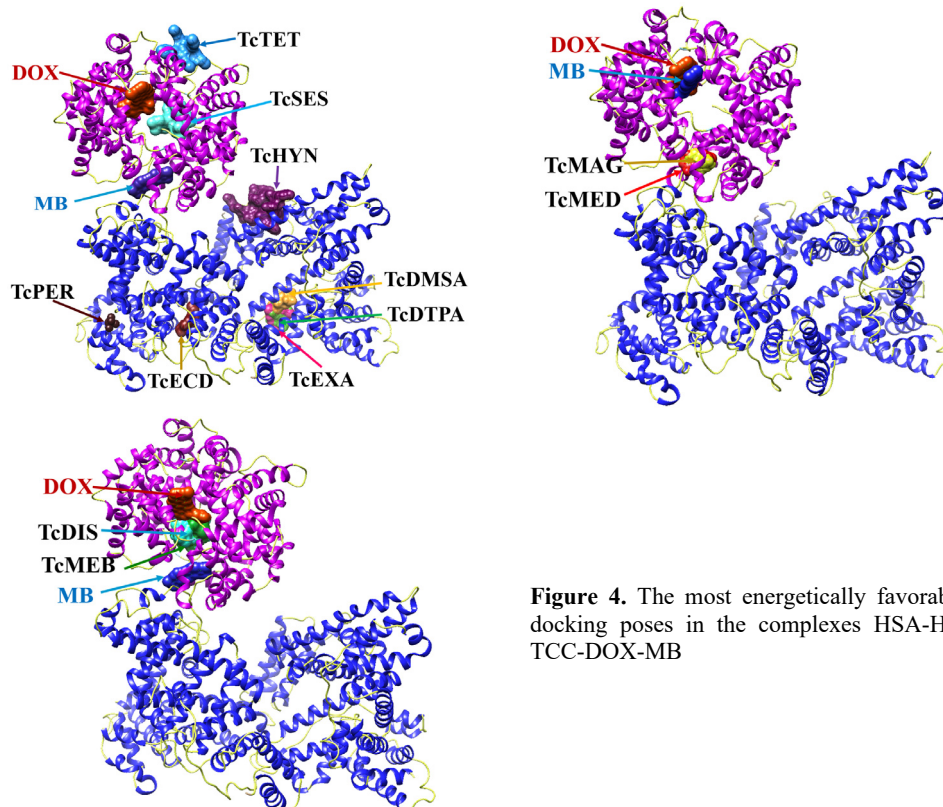


Figure 4. The most energetically favorable docking poses in the complexes HSA-Hb-TCC-DOX-MB

Taken together, these results highlight the transformative role of Hb when integrated with albumin in protein-based carriers. By expanding the available binding landscape, Hb improves affinity for key radiopharmaceuticals (notably TcMEB and TcDIS), provides exclusive and stable pockets for DOX, and preferentially anchors fluorescent dyes. The observed behavior of ligands within the hybrid nanosystems suggest that albumin primarily stabilizes technetium-based radiopharmaceuticals, while hemoglobin serves as the dominant host for DOX and NIR dyes. Such separation may optimize loading efficiency, minimize interference between ligands, and allow simultaneous therapeutic and diagnostic functions.

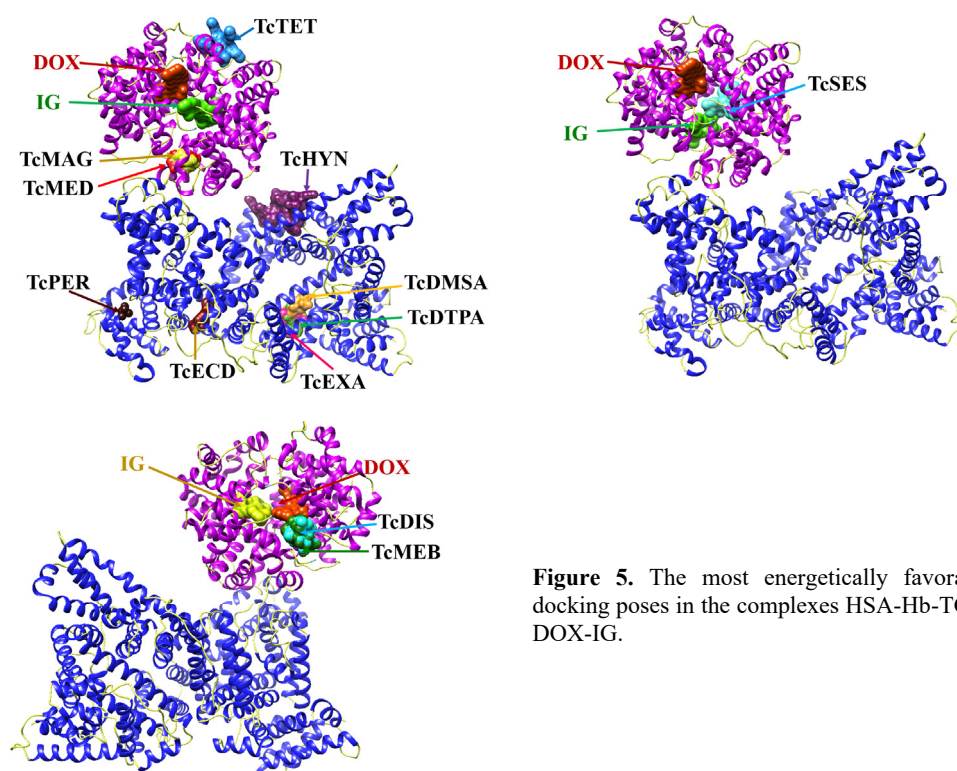


Figure 5. The most energetically favorable docking poses in the complexes HSA-Hb-TCC-DOX-IG.

From a clinical standpoint, HSA–Hb hybrids may offer several advantages over existing platforms. Intrinsic oxygen transport properties of Hb could modulate drug release in hypoxic tumors, addressing one of the most intractable barriers in chemotherapy. The preferential fluorophore binding observed for Hb also suggests superior fluorescence imaging capabilities, which are crucial for real-time surgical navigation and longitudinal monitoring of drug biodistribution. Finally, the strong and specific interactions predicted computationally provide a rationale for experimental development of HSA-Hb carriers as theranostic systems.

Future work should focus on validating these computational findings through experimental assays, including in vitro binding studies, cellular uptake analyses, and in vivo biodistribution imaging. Additionally, the potential immunogenicity and metabolic fate of hemoglobin-based carriers warrant careful evaluation to ensure clinical viability.

CONCLUSIONS

In conclusion, the present study demonstrates that hybrid assemblies of human serum albumin and hemoglobin (HSA-Hb) provide a versatile platform for doxorubicin delivery with integrated radionuclide and fluorescence imaging functionalities. Computational docking revealed that hemoglobin significantly expands the binding landscape, enabling preferential and stronger interactions with several technetium-99m radiopharmaceuticals while also serving as the dominant binding site for both doxorubicin and near-infrared fluorophores. This redistribution of ligand affinities between albumin and hemoglobin reduces competition for binding pockets and allows simultaneous incorporation of therapeutic and diagnostic agents within a single carrier. The spatial separation of ligands across albumin and hemoglobin subunits suggests a functional complementarity that could enhance drug stability, facilitate controlled release under tumor-specific conditions, and improve imaging contrast for multimodal theranostics. Taken together, our findings highlight HSA-Hb systems as promising candidates for the rational design of next-generation protein-based nanocarriers that combine therapeutic efficacy with real-time monitoring, paving the way for their further experimental validation and translational development.

Acknowledgements

This work was supported by the Ministry of Education and Science of Ukraine (Project No. ДЗ/174-2025).

ORCID

Valeriya Trusova, <https://orcid.org/0000-0002-7087-071X>; Uliana Malovytsia, <https://orcid.org/0000-0002-7677-0779>
Galyna Gorbenko, <https://orcid.org/0000-0002-0954-5053>; Andrey Zelinsky, <https://orcid.org/0000-0002-4110-8523>
Borys Borts, <https://orcid.org/0000-0002-1492-4066>; Pylyp Kuznietsov, <https://orcid.org/0000-0001-8477-1395>
Ivan Yakymenko, <https://orcid.org/0000-0002-0194-8376>

REFERENCES

- [1] C. Ferraro, M. Dattilo, F. Patitucci, S. Prete, G. Scopelliti, O. Parisi, and F. Puoci, *Pharmaceutics*, **16**, 1172 (2024). <https://doi.org/10.3390/pharmaceutics16091172>
- [2] J. Gao, J. Karp, R. Langer, and N. Joshi, *Chem Mater.* **35**, 359 (2023). <https://doi.org/10.1021/acs.chemmater.2c03003>
- [3] A. Prajapati, E. Garcia-Garrido, and A. Somoza, *Cancers (Basel)*. **13**, 3011 (2021). <https://doi.org/10.3390/cancers13123011>
- [4] A. Spada, J. Emami, J. Tuszynski, and A. Lavasanifar, *Mol. Pharmaceut.* **18**, 1862 (2021). <https://doi.org/10.1021/acs.molpharmaceut.1c00046>
- [5] V. Trusova, U. Tarabara, I. Karnaukhov, A. Zelinsky, B. Borts, I. Ushakov, L. Sidenko, and G. Gorbenko, *East Eur. J. Phys.* (4), 447 (2024). <https://doi.org/10.26565/2312-4334-2024-4-54>
- [6] V. Trusova, U. Malovytsia, P. Kuznietsov, I. Karnaukhov, A. Zelinsky, B. Borts, I. Ushakov, L. Sidenko, and G. Gorbenko, *East Eur. J. Phys.* (1), 376 (2025). <https://doi.org/10.26565/2312-4334-2025-1-46>
- [7] V. Trusova, U. Malovytsia, P. Kuznietsov, I. Karnaukhov, A. Zelinsky, B. Borts, I. Ushakov, L. Sidenko, and G. Gorbenko, *East Eur. J. Phys.* (2), 398 (2025). <https://doi.org/10.26565/2312-4334-2025-2-48>
- [8] J. Lukin, and C. Ho, *Chem. Rev.* **104**, 1219 (2004). <http://dx.doi.org/10.1021/cr940325w>
- [9] M.F. Adasme, K.L. Linnemann, S.N. Bolz, F. Kaiser, S. Salentin, V.J. Haupt, and M. Schroeder, *Nucl. Acids Res.* **49**, W530-W534 (2021). <https://doi.org/10.1093/nar/gkab294>

КОМП'ЮТЕРНЕ ДОСЛІДЖЕННЯ СИСТЕМ ДОСТАВКИ ЛІКІВ З РАДІОНУКЛІДНИМИ ТА ФЛЮОРЕСЦЕНТНИМИ МОДАЛЬНОСТЯМИ ВІЗУАЛІЗАЦІЇ.

IV. СИСТЕМИ НА ОСНОВІ АЛБУМІНУ ТА ГЕМОГЛОБІНУ ДЛЯ ДОСТАВКИ ДОКСОРУБІЦИНУ

В. Трусова^a, У. Маливиця^a, П. Кузнєцов^b, І. Якименко^b, І. Карнаухов^c, А. Зелінський^c, Б. Борц^c,
І. Ушаков^c, Л. Сіденко^c, Г. Горбенко^a

^aКафедра медичної фізики та біомедичних нанотехнологій, Харківський національний університет імені В.Н. Каразіна
м. Свободи 4, Харків, 61022, Україна

^bКафедра фізики ядра та високих енергій імені О.І. Ахієзера, Харківський національний університет імені В.Н. Каразіна
м. Свободи 4, Харків, 61022, Україна

^cНаціональний науковий центр «Харківський фізико - технічний інститут», Харків, вул. Академічна, 1, 61108, Україна
Розробка мультифункціональних систем доставки лікарських засобів, що поєднують терапевтичні та діагностичні можливості, залишається одним із ключових викликів сучасної онкології. У даній роботі досліджено гібридні носії на основі

сироваткового альбуміну людини та гемоглобіну (HSA-Hb) для доставки доксорубіцину (DOX), що містили радіонуклідні та флуоресцентні молекули-репортери. За допомогою методу молекулярного докінгу було проаналізовано взаємодію комплексів HSA-Hb із дванадцятьма радіофармпрепаратами на основі технецію-99m (^{99m}Tc), DOX та чотирма барвниками ближньої інфрачервоної (NIR) області. Результати показали, що гемоглобін суттєво розширює спектр зв'язування, забезпечуючи унікальні та високоафінні сайти для кількох комплексів ^{99m}Tc (зокрема TcMEB та TcDIS), а також виступає основним матричним білком для DOX і NIR-барвників. Усередині субодиниць Hb були ідентифіковані два окремі сайти зв'язування DOX, що вказує на підвищену стабільність препарату та потенційну чутливість до гіпоксії пухлин. Флуоресцентні барвники, включно з метиленовим синім, індоціаніновим зеленим, AK7-5 та SQ1, демонстрували переважне зв'язування з Hb із більшою спорідненістю, ніж до альбуміну, що свідчить про кращу придатність для оптичної візуалізації. Важливо, що афінність радіофармпрепаратів до альбуміну, а терапевтичних та діагностичних агентів – до гемоглобіну знижувала конкуренцію за сайти зв'язування та забезпечувала одночасну інтеграцію мультимодальних функцій в межах однієї наноплатформи. Отримані результати свідчать, що HSA-Hb наноносії є перспективними кандидатами для створення новітніх тераностичних платформ, що поєднують ефективну доставку DOX з неінвазивним радіонуклідним та флуоресцентним моніторингом.

Ключові слова: *наносистеми доставки ліків на основі білків; людський сироватковий альбумін; гемоглобін; доксорубіцин; комплекси технецію; інфрачервоні барвники; молекулярний докінг*